

# The vanishing water/oil interface in the presence of antagonistic salt

Gudrun Glende,<sup>1</sup> Astrid S. de Wijn,<sup>1,2</sup> and Faezeh Pousaneh\*<sup>1</sup>

<sup>1</sup>*Department of Mechanical and Industrial Engineering,  
Norwegian University of Science and Technology, 7491 Trondheim, Norway*

<sup>2</sup>*Department of Physics, Stockholm University, Sweden*

Antagonistic salts are salts which consist of hydrophilic and hydrophobic ions. In a binary mixture of water and organic solvent, these ions preferentially dissolve into different phases. We investigate the effect of an antagonistic salt, tetraphenylphosphonium chloride  $\text{PPh}_4\text{Cl}$ , in a mixture of water and 2,6-lutidine by means of Molecular Dynamics (MD) Simulations. For increasing concentrations of the salt the two-phase region is shrunk and the interfacial tension is reduced, in contrast to what happens when a normal salt is added to such a mixture. The MD simulations allow us to investigate in detail the mechanism behind the reduction of the surface tension. We obtain the ion and composition distributions around the interface and determine the hydrogen bonds in the system and conclude that the addition of salt alter the hydrogen bonding.

## I. INTRODUCTION

Mixtures of water and oil are ubiquitous in nature and technology. Biological systems are largely water-based, but also contain oily molecules. In maritime and other off-shore applications, lubricants and other oils come into contact with seawater often. What many of these mixtures have in common is the additional presence of salt ions. This addition of a small amount of salt can significantly change the properties of an oil/water mixture.

Most binary mixtures of water and organic molecules are phase-separated at ambient conditions. When a simple inorganic salt is added to the mixture, the two-phase region enlarges [1]. This picture changes for more complex salts with organic groups that are hydrophobic. When an antagonistic (or amphiphilic) salt is added to an oil/water mixture this can lead to reduction of interfacial tension between water and oil, and therefore to a shrinkage of the two phase region. It has been shown experimentally that the interfacial tension decreases with increasing the amount of antagonistic salts [2]. If enough salt is added, it can even make the interface disappear altogether and cause the oil and water to mix [3–7]. In addition to changes in the interfacial tension, adding an antagonistic salt can also lead to interesting structural changes, such as a lamellar phases [3, 5, 6]. These effects have been studied and explained theoretically for small salt concentration [8] and for higher salt concentrations [9–11]. Analytical calculations of the ion distribution have suggested that the cations and anions of an antagonistic salt tend to adsorb around a water-oil interface [12].

Here we study this problem in a different way, using detailed atomistic Molecular Dynamics (MD) simulations. Because such simulations give us the trajectories of all the particles in the system, they can be used as numerical experiments. They allow us to

observe in much more detail where the ions are and how they are behaving, which enables us to study and verify the mechanisms of the reduction in the interfacial tension. We investigate a mixture of water and 2,6-lutidine (2,6-dimethylpyridin) with various concentrations of the antagonistic salt tetraphenylphosphonium chloride  $\text{PPh}_4^+\text{Cl}^-$ , with hydrophilic anion  $\text{Cl}^-$  and ( $\text{PPh}_4^+$ ) anion.

The phase diagram and mixing behaviour of neat water/2,6-lutidine mixtures have gained considerable attention in the context of colloidal systems [13–15] and critical Casimir forces [16, 17]. Critical Casimir forces rises between two selective (hydrophilic or hydrophobic) colloids in a suspension when the liquid base of the suspension is near its critical point [18, 19]. When colloids are charged the force is tuned by electrostatic interactions [16, 17, 20–25]. Moreover, the addition of a salt to the water/2,6-lutidine mixture allows one to tune these interactions and create different structures [3, 5, 6, 9]. Antagonistic salts are of particular interest in this context, because the two ions have substantially different interactions with the oil and water.

The neat water/2,6-lutidine binary mixture and its phase diagram have been studied experimentally and analytically [26, 27] and recently by molecular dynamics simulations [28]. Without the additional salt, this mixture has a closed-loop phase diagram with a relatively wide temperature miscibility gap, which makes it very suitable for studying (de)mixing. The lower critical point is close to room temperature, around  $T_c \approx 307.1$  K with the lutidine mole fraction  $x_{lut} \approx 6.1\%$  [26].

An antagonistic salt has one hydrophilic ion and one hydrophobic ion. This makes them potentially very different from more simple hydrophilic salts, where both cation and anion are hydrophilic. With the addition of such hydrophilic salts, the solubility of water and the organic solvent decreases and therefore the two-phase region is enhanced. Rather than both ions preferring to dissolve in water, in antagonistic salts, one ion will prefer to dissolve in the water, while the other prefers to dissolve in the oil. The effect of the antagonistic salt  $\text{Na}^+\text{BPh}_4^-$  on a binary mixture of  $\text{D}_2\text{O}$  and 3-methylpyridine (3MP) was

---

\*Corresponding author.  
faezeh.pousaneh@ntnu.no.

Electronic address:

recently studied experimentally by Sadakane *et al.* [3, 5] by means of small-angle neutron scattering and optical microscopy. They show that for increasing salt concentration the two-phase region shrinks and eventually even disappears. A similar effect has been reported with the salt  $\text{PPh}_4^+\text{Cl}^-$  [7] (see Fig. 1 (right)) that we study in this work. The hydrophobic cation has four phenyl rings that interfere with hydrogen bonding and the hydration shell. Thus, the cations preferentially dissolve in an organic solvent (oil) whereas the anions prefer to stay within the water. Consequently, the cations and anions behave antagonistically and may distribute heterogeneously when added to a binary liquid consisting of water and an organic solvent.

In this article, we study the effect of an antagonistic salt, tetraphenylphosphonium chloride  $\text{PPh}_4\text{Cl}$ , in a mixture of water and 2,6-lutidine by means of atomistic MD Simulations. We investigate the addition of salt on properties of the mixture, such as surface tension and hydrogen bonds.

The organization of this paper is as follows. In Sec. II we explain the MD simulations setup and models for the water and 2,6-lutidine mixture with the antagonistic salt  $\text{PPh}_4\text{Cl}$ . Section. III gives and discusses the simulation results, which is divided into two subsections, concentration profiles III A, surface tension and hydrogen bonds III B. We conclude the paper in Sec. IV.

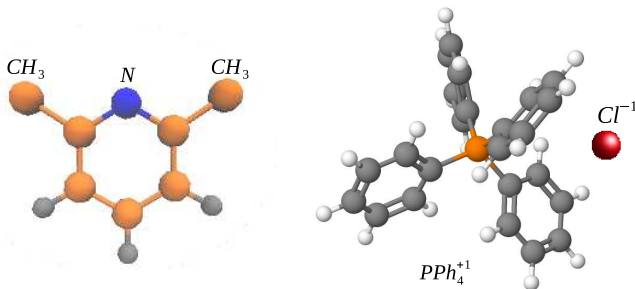


FIG. 1: (Left) Schematic representation of the 2,6-lutidine molecule,  $\text{C}_7\text{H}_9\text{N}$ .  $\text{CH}_3$  groups are shown as single united atoms. For the charge distributions see ref. [28]. (Right) Schematic representation of salt  $\text{Ph}_4^+\text{Cl}^-$ . Cation is tetraphenylphosphonium  $\text{PPh}_4^+$  with four phenyl rings, where the orange atom in the middle represents the phosphonium. The anion is  $\text{Cl}^-$ .

## II. SIMULATION SETUP

In this work, we consider the same mixture of water/2,6-lutidine provided in [28]. For the organic molecule 2,6-lutidine we use the recent parametrisation [28] developed using the Gromacs package [29]. The model successfully captures the lutidine bulk properties and the lutidine/water binary mixture properties, such as the phase diagram, critical properties and surface tension. We therefore choose the same topology and charge

distributions for the lutidine molecule as in [28]. The lutidine molecule  $\text{C}_7\text{H}_9\text{N}$  is presented by 11 atoms with the  $\text{CH}_3$  groups as united atoms, Fig. 1 (left). For the charge distributions on the lutidine see [28].

All simulations in this work are performed using the Gromacs/2016 MD simulation package [29]. The Gromos54a7 forcefield [30] is used for almost all interactions. Bond lengths are kept fixed at the Gromos54a7 equilibrium length, using the LINCS algorithm [31]. Water is described using the TIP4P/2005 model. For the lutidine molecules, the partial charges and dihedrals are taken from [28]. The Particle Mesh Ewald (PME) approach is applied to the electrostatic interactions beyond a 1.2 (nm) cutoff. A cut-off length of 1.2 (nm) is applied to the van der Waals interactions.

Simulations are performed in the NPT ensemble. The temperature is controlled by a V-rescale thermostat at  $T = 380$  K, and the pressure is controlled by a Parrinello-Rahman barostat (isotropic,  $p = 1$  atm). At  $T = 380$  K the mixture is in the phase separated region [28].

For the binary mixture, we simulate a box containing 19000 water molecules and 3000 lutidine molecules. This corresponds to 13% mole fraction of lutidine. The initial box size is (7, 7, 19) nm, see Fig. 2 (top). The simulation time step is 2 fs. We run the simulation for 500 ns to equilibrate the system and allow the water and lutidine to phase separate. The equilibrated configuration is shown in Fig. 2 (bottom).

Next, we add the antagonistic salt to the mixture. We obtain the topology for the antagonistic salt  $\text{PPh}_4^+\text{Cl}^-$  using the Automatic Topology Builder [32] for the Gromos54a7 forcefield, see Fig. 1 (right). In order to investigate the effect of salt on interfacial tension of water/lutidine mixture, we simulate six different systems with different salt concentration from 0.045% to 2.70% mole fractions of salt. For every salt ion we add the the box, we remove one water molecule. We then run the simulations for up to 600 ns depending on the system. Equilibrium typically is reached around 200-300 ns. We verify that the system has reached equilibrium not only by checking density, pressure, and temperature, but also the structural properties such as partial densities, radial distribution functions and hydrogen bonds.

## III. RESULTS

Examples of equilibrated water/2,6-lutidine/salt configurations are shown in Fig. 3. From the snapshots, it can be seen that the salt tends to locate around the interface. As the concentration increases, the interface becomes saturated and the salt ions are present deeper into the bulk of the water and lutidine. Finally, at the extremely high concentration of 2.70% mole fraction the interface disappears completely and the water and lutidine are mixed.

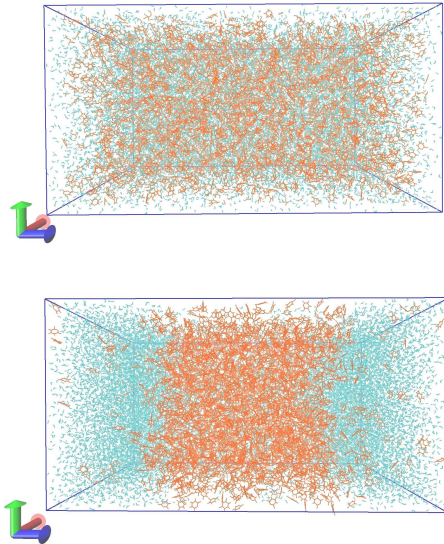


FIG. 2: (Top) the initial configuration of water/2,6-lutidine box, (bottom) simulation result after 500 ns at  $T = 380$  K. Blue color molecules indicate water molecules and the ring orange-coloured indicate lutidine molecules.

### A. Concentration profiles

We have investigated the concentration profiles in more detail. We first focus on lutidine mole fractions in both phases, lutidine-rich and lutidine-poor. Fig. 4 shows the lutidine mole fractions as a function of the position in the box, obtained from simulations. One can see that for higher salt concentrations, the interface between two phases become softer. At the highest concentration, the system becomes homogeneous with water and lutidine mixed. The concentration values in the two phases, water-rich and lutidine-rich can be obtained from the classical theories for interfaces between coexisting phases,

such as Cahn and Hilliard or Landau-Ginzburg theory, which both predict a hyperbolic-tangent shaped interfacial density profile [28, 33–35]:

$$w_{\text{lut}}(z) = w_{\text{lut}}^{\text{p}} + \frac{w_{\text{lut}}^{\text{r}} - w_{\text{lut}}^{\text{p}}}{2} \left[ \tanh\left(\frac{z - z_0 + c}{\lambda}\right) - \tanh\left(\frac{z - z_0 - c}{\lambda}\right) \right], \quad (1)$$

with  $w_{\text{lut}}^{\text{r}}$  and  $w_{\text{lut}}^{\text{p}}$  the fractions of 2,6-lutidine in the lutidine-rich and lutidine-poor phases respectively. The width of the interface is given by  $\lambda$ .  $c$  is the half-width of the lutidine-rich region, and  $z_0$  is the center of the lutidine-rich phase. We fit the concentration profiles from the simulations to this function. These fits are indicated by the solid lines in Fig. 4. The fit parameters obtained for the lutidine mole fractions in the rich and poor phases are shown in Fig. 5 and given in the appendix. The values indicate that with increasing the salt concentration the lutidine mole fraction in the lutidine-rich phase decreases, while it increases in the lutidine-poor phase.

Next, we study the ion concentrations in the two phases and near the interfaces. Fig. 6 shows ion concentrations obtained from simulation. The top figure shows the  $\text{PPh}_4^+$  mole fractions and the bottom one shows the  $\text{Cl}^-$  mole fractions. There are clear concentration peaks around the interface between water and lutidine, rather than each ion staying at its preferred phase (hydrophilic anion into water and hydrophobic cations into lutidine). At extremely high salt concentration, when the water and lutidine are mixed, the salt concentration becomes homogeneous. In order to obtain the concentration values of  $\text{PPh}_4^+$  in each phase, we fit the concentration profiles to the modified hyperbolic-tangent function from Cahn and Hilliard theory. The modified function corresponds to an asymmetric interface where the three concentrations, at the interface,  $w^{\text{m}}$ , and in the two phases,  $w^{\text{r}}, w^{\text{l}}$ , next to the interface, are different. The function is

$$w(z) = \frac{(w^{\text{l}} + w^{\text{r}})}{2} - \left[ \frac{\tanh(c/\lambda)[w^{\text{l}} - w^{\text{r}}] + [w^{\text{l}} + w^{\text{r}} - 2w^{\text{m}}]}{4 \tanh(c/\lambda)} \right] \tanh\left(\frac{z - z_0 + c}{\lambda}\right) - \left[ \frac{\tanh(c/\lambda)[w^{\text{l}} - w^{\text{r}}] - [w^{\text{l}} + w^{\text{r}} - 2w^{\text{m}}]}{4 \tanh(c/\lambda)} \right] \tanh\left(\frac{z - z_0 - c}{\lambda}\right), \quad (2)$$

where  $w^{\text{r}}, w^{\text{l}}$  and  $w^{\text{m}}$  are the three concentrations. The solid lines in Fig. 6 (top) show the fittings to the last equation. They indicate that with increasing salt concentration the amount of ions around the interfaces increases. This can be better seen in Fig. 7. The fit parameters are also given in the appendix.

We furthermore show the charge density profile in

Fig. 8. The figure illustrates that the positive and negative charges pile up when the salt concentration is increased up to a point. However, at large salt concentrations they become uniformly distributed due to mixing in the system.

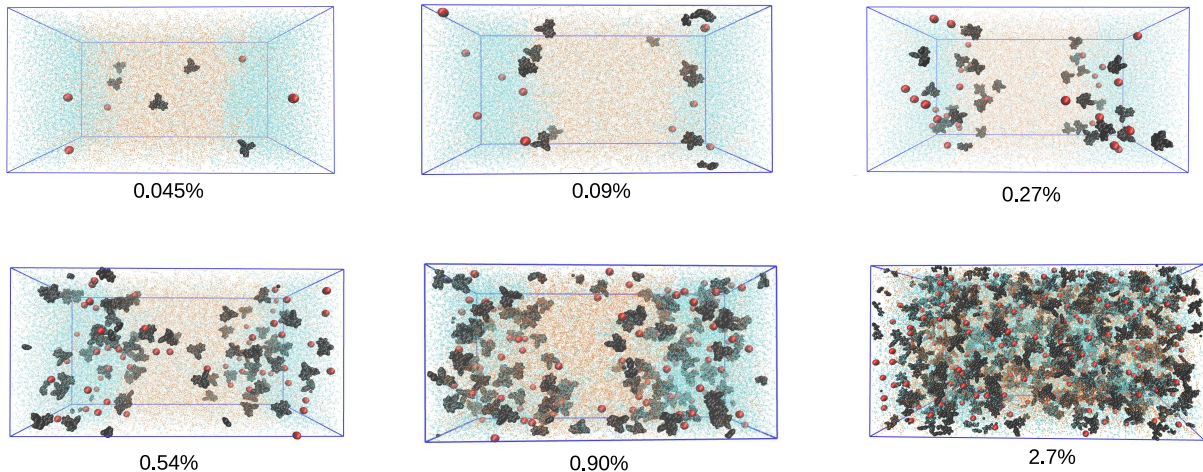


FIG. 3: Equilibrated configurations of the water/2,6-lutidine systems with different salt concentrations. Red spherical particles indicate the  $\text{Cl}^-$  anion and black bigger particles indicate  $\text{PPh}^+$  cations. The salt concentrations are indicated below each figure. At lower concentrations, the ions predominantly sit around the interface, but at the highest concentration the interface disappears and the system is mixed.

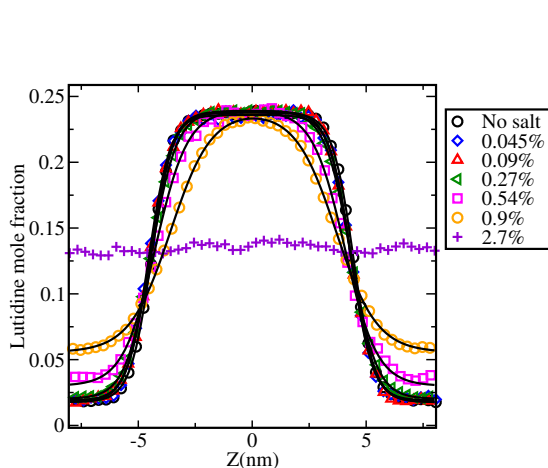


FIG. 4: Mole fraction of lutidine at different salt concentrations as a function of position in the simulation box along the axis perpendicular to the interfaces.

### B. Interfacial tension

In order to obtain the interfacial tension we continue the simulations in the NPT ensemble using a Brendsen barostat for 200 ns. In Gromacs, the average interfacial tension  $\gamma$  can be calculated directly from the difference between the normal and lateral pressure

$$\gamma(t) = \frac{1}{n} \int_0^{L_z} \left[ P_{zz}(z, t) - \frac{P_{xx}(z, t) + P_{yy}(z, t)}{2} \right] dz, \quad (3)$$

where  $L_z$  is the height of the box and  $n$  is the number of surfaces. The results are plotted in Fig. 9. The error estimates for the averages are obtained based on block

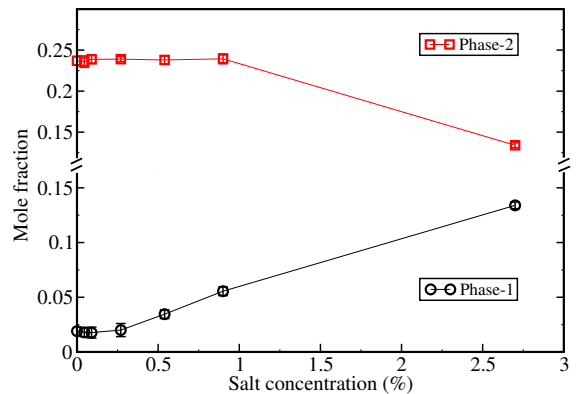


FIG. 5: Lutidine mole fraction in two phases, phase-1 (lutidine-poor) and phase-2 (lutidine-rich) obtained from fitting to Eq. 2.

averages. We can see a clear reduction of interfacial tension with increasing salt concentration.

To further investigate the effect of antagonistic salt in the mixture, we now focus on the hydrogen bonds between lutidine and water. We obtain the number of hydrogen bonds between water-lutidine molecules, and between water-water molecules using Gromacs. Hydrogen bonds are determined based on cutoffs for the angle Hydrogen-Donor-Acceptor and the distance Donor-Acceptor. O and N are acceptor here [29]. The results are plotted in Fig. 10 for different salt concentrations. The number of hydrogen bonds between water and water decreases with increasing salt concentration, while the number of hydrogen bonds between water and lutidine increases. That is a clear indication of the mixing of the water and lutidine. The error estimate of the averages

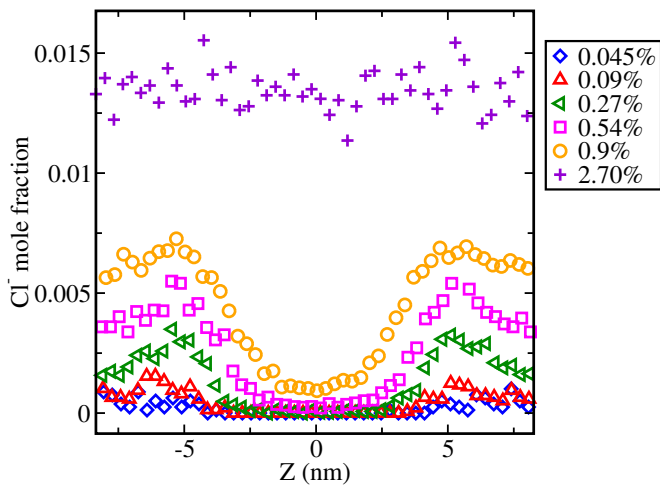
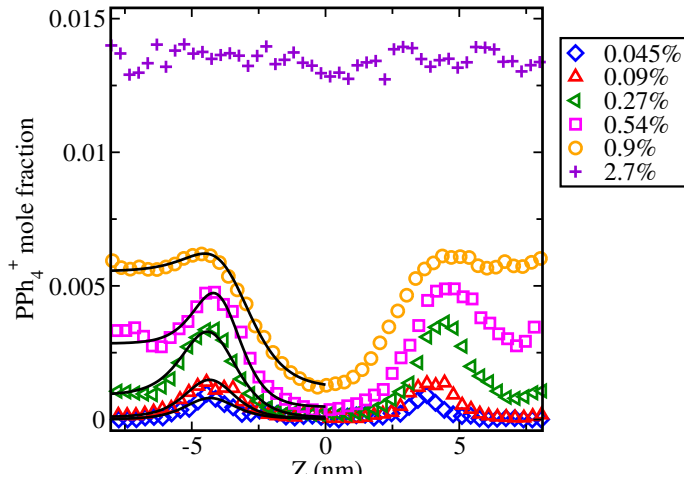


FIG. 6: The mole fractions of  $\text{PPh}_4^+$  (top) and  $\text{Cl}^-$  (bottom) for different salt concentrations as a function of position in the simulation box along the axis perpendicular to the interfaces.

are obtained based on block averages.

#### IV. CONCLUSION

The addition of antagonistic salt tetraphenylphosphonium chloride  $\text{PPh}_4\text{Cl}$  in water/2,6-lutidine has been studied by Molecular Dynamics Simulations. The salt has hydrophilic anion and hydrophobic cation, therefore different affinity with the water and lutidine phases. We have examined how the salt effects on the mixture properties. We study the concentration of all four components, we determine that the ions tend to stay around the interface of the two phases. However, the ion concentration profiles in both phases become the same at a high value of salt concentration. Thus, our simulations reveal that by increasing the salt concentration the two-phase region start to shrink and finally at a high salt concentration,

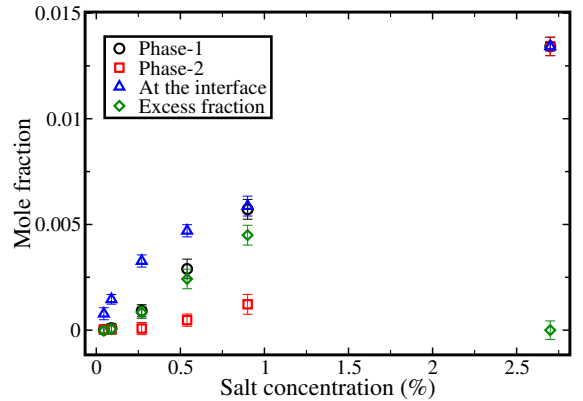


FIG. 7:  $\text{PPh}_4^+$  mole fraction in different phases, phase-1 (lutidine-poor) and phase-2 (lutidine-rich) and at the interface obtained from fitting to Eq. 2. The excess mole fraction of cation between two phases are also shown in green-diamond data

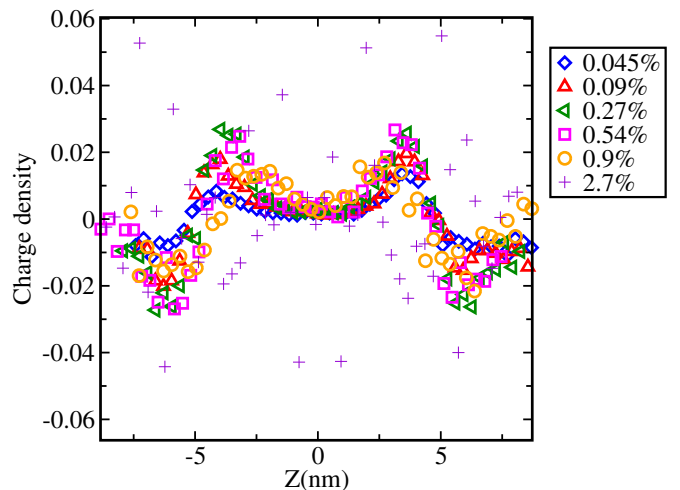


FIG. 8: Charge number density for different salt concentrations as a function of position in the simulation box along the axis perpendicular to the interfaces.

water and lutidine mixes.

We obtain surface tension between water and lutidine phases, and show that it decreases by increasing the salt concentration. We further investigate the hydrogen bonds between water and lutidine molecules. We report that with increasing the salt concentration, the number of hydrogen bonds between water-water molecules decreases while the number of hydrogen bonds between water-lutidine increases. This can be one of the indications for the water and lutidine mixing.

It would be interesting to investigate the possibility of mesophases before and after mixing as well as the structure of the mixed phase [36, 37]. However, such a study would necessitate a much bigger system than the one we have simulated here. We are limited in the system size by the computational power required for the detailed atom-

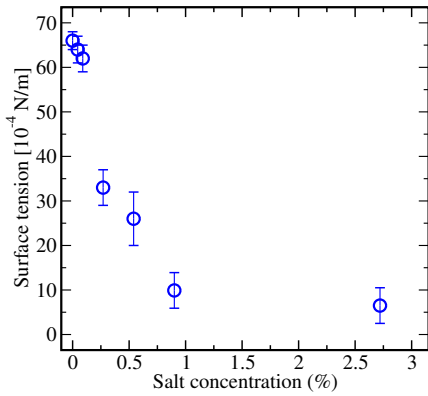


FIG. 9: Interfacial tension per interface in systems with different salt concentration. Interfacial tension decreases by increasing

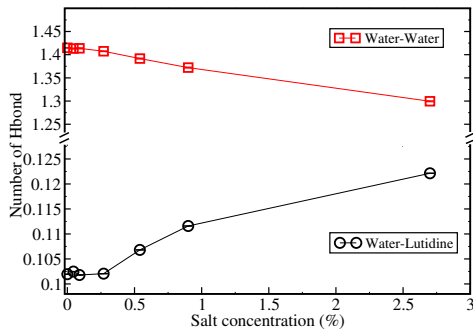


FIG. 10: Number of hydrogen bonds between water-water and water-lutidine molecules (per water molecule) in systems with different salt concentration.

istic description of the molecules.

### Acknowledgements

The work has been supported by National Infrastructure for Computational Science in Norway (UNINETT Sigma2) with computer time for the Center for High Per-

formance Computing (NN9573K and NN9572K). The authors acknowledge The Research Council of Norway for NFR project number 275507 for financial support.

### V. APPENDIX. A

The fit parameters obtained for the lutidine and  $\text{PPh}_4^+$  mole fractions in the rich and poor phases are given in Tables. I and II, respectively.

Salt	Phase-1	Phase-2
No salt	$0.019 \pm 0.004$	$0.237 \pm 0.008$
0.045%	$0.0179 \pm 0.004$	$0.236 \pm 0.007$
0.09%	$0.0177 \pm 0.004$	$0.238 \pm 0.005$
0.27%	$0.020 \pm 0.006$	$0.239 \pm 0.003$
0.54%	$0.0345 \pm 0.004$	$0.238 \pm 0.005$
0.90%	$0.055 \pm 0.004$	$0.239 \pm 0.006$
2.70%	$0.134 \pm 0.003$	$0.134 \pm 0.003$

TABLE I: Lutidine mole fractions at two phases, lutidine-poor (phase-1) and lutidine-rich (phase-2), for systems with different salt concentrations.

Salt	Phase-1	Phase-2	At the interface
0.045%	$0.0014 \pm 0.0004$	$0.0037 \pm 0.0002$	$0.077 \pm 0.003$
0.09%	$0.009 \pm 0.0002$	$0.004 \pm 0.0002$	$0.14 \pm 0.01$
0.27%	$0.091 \pm 0.003$	$0.0076 \pm 0.0003$	$0.32 \pm 0.03$
0.54%	$0.28 \pm 0.06$	$0.047 \pm 0.003$	$0.46 \pm 0.06$
0.90%	$0.57 \pm 0.08$	$0.122 \pm 0.04$	$0.58 \pm 0.04$
2.70%	$1.34 \pm 0.2$	$1.34 \pm 0.2$	$1.34 \pm 0.2$

TABLE II:  $\text{PPh}_4^+$  mole fractions at two phases, lutidine-poor (phase-1) and lutidine-rich (phase-2), and at the interface, for systems with different salt concentrations. The values are given in unit of  $10^{-3}$ .

- 
- [1] V. Balevicius and H. Fuess *Phys. Chem. Chem. Phys.*, vol. 1, pp. 1507–1510, 1999.
- [2] G. Luo, S. Malkova, J. Yoon, D. G. Schultz, B. Lin, M. Meron, I. Benjamin, P. Vanýsek, and M. L. Schlossman *Science*, vol. 311, pp. 216–218, 2006.
- [3] K. Sadakane, M. Nagao, H. Endo, and H. Seto *Chem. Lett.*, vol. 139, p. 234905, 2013.
- [4] K. Sadakane, A. Onuki, K. Nishida, S. Koizumi, and H. Seto *Soft Matter*, vol. 7, p. 1334, 2011.
- [5] K. Sadakane, A. Onuki, K. Nishida, S. Koizumi, and H. Seto *Phys. Rev. Lett.*, vol. 103, p. 167803, 2009.
- [6] J. Leys, D. Subramanian, E. Rodezno, B. Hammouda, and M. A. Anisimov *Soft Matter*, vol. 9, p. 9326, 2013.
- [7] K. Sadakane, Y. Horikawa, M. Nagao, and H. Seto *Chem. Lett.*, vol. 41, p. 1075–1077, 2012.
- [8] A. Onuki and H. Kitamura *J. Chem. Phys.*, vol. 121, p. 3143, 2004.
- [9] F. Pousaneh and A. Ciach *Soft Matter*, vol. 10, pp. 8188–8201, 2014.
- [10] A. Onuki, T. Araki, and R. Okamoto *Phys. Rev. Lett.*, vol. 23, p. 284113, 2011.
- [11] A. Onuki and R. Okamoto *Curr. Opin. Colloid Interface Sci.*, vol. 16, p. 525, 2011.
- [12] A. Onuki *Phys. Rev. E*, vol. 73, p. 021506, 2006.
- [13] M. L. Broide, Y. Garrabos, and D. Beysens *J. Chem. Phys.*, vol. 47, p. 3768, 1993.

- [14] B. J. Frisken, F. Ferri, and D. S. Cannel *Phys. Rev. Lett*, vol. 66, p. 2754, 1991.
- [15] P. D. Gallagher and J. M. Maher *Phys. Rev. A*, vol. 46, p. 2012, 1992.
- [16] A. Gambassi, A. Maciołek, C. Hertlein, U. Nellen, L. Helden, C. Bechinger, and S. Dietrich *Phys. Rev. E*, vol. 80, p. 061143, 2009.
- [17] C. Hertlein, L. Helden, A. Gambassi, S. Dietrich, and C. Bechinger *Nature*, vol. 451, p. 172, 2008.
- [18] M. E. Fisher and P. G. de Gennes *C. R. Acad. Sci. Paris B*, vol. 287, p. 207, 1978.
- [19] M. Krech *J. Phys.:Cond. Mat*, vol. 11, p. R391, 1999.
- [20] U. Nellen, L. Helden, and C. Bechinger *Europhys Lett*, vol. 88, p. 26001, 2009.
- [21] U. Nellen, J. Dietrich, L. Helden, S. Chodankar, K. Nygard, J. F. van der Veen, and C. Bechinger *Soft Matter*, vol. 80, p. 061143, 2011.
- [22] M. Bier, A. Gambassi, M. Oettel, and S. Dietrich *Europhys Lett*, vol. 95, p. 60001, 2011.
- [23] F. Pousaneh and A. Ciach *J. Phys.:Cond. Mat*, vol. 23, p. 412101, 2011.
- [24] F. Pousaneh, A. Ciach, and A. Maciołek *Soft Matter*, vol. 8, pp. 7567–7581, 2012.
- [25] F. Pousaneh, A. Ciach, and A. Maciołek *Soft Matter*, vol. 10, pp. 470–483, 2014.
- [26] R. J. L. Andon and J. D. Cox *J. Chem. Soc.*, vol. 1, pp. 4601–4606, 1952.
- [27] Y. Jayalakshmi, J. S. V. Duijneveldt, , and D. Beysens *J. Chem. Phys*, vol. 100, p. 604, 1993.
- [28] F. Pousaneh, O. Edholm, and A. Maciołek *J. Chem. Phys*, vol. 145, p. 014501, 2016.
- [29] D. van der Spoel, E. Lindahl, B. Hess, G. Groenhof, A. E. Mark, and H. J. Berendsen *J. Comput. Chem.*, vol. 26, pp. 1701–1718, 2005.
- [30] N. Schmid, A. P. Eichenberger, A. Choutko, S. Riniker, M. Winger, A. E. Mark, , and W. F. van Gunsteren *Eur. Biophys. J.*, vol. 40, pp. 843–856, 2011.
- [31] B. Hess, H. Bekker, H. J. C. Berendsen, and J. G. E. M. Fraaije *J. Comput. Chem.*, vol. 18, p. 1463–1472, 1997.
- [32] A. K. Malde, L. Zuo, M. Breeze, M. Stroet, D. Poger, P. C. Nair, C. Oostenbrink, and A. E. Mark *J. Chem. Theory Comput.*, vol. 7, p. 4026–4037, 2011.
- [33] J. W. Cahn and J. E. Hilliard *J. Chem. Phys*, vol. 28, p. 258, 1958.
- [34] G. A. Chapela, G. Saville, S. M. Thompson, and J. S. Rowlinson *J. Chem. Soc., Faraday Trans.*, vol. 2, p. 1133, 1977.
- [35] K. Binder, M. Bowker, J. E. Inglesfield, and P. J. Rous, *Cohesion and Structure of Surfaces*. The Netherlands: Elsevier Science, 1995.
- [36] N. Tasios, S. Samin, R. van Roij, and M. Dijkstra *Phys. Rev. Lett*, vol. 119, p. 218001, 2017.
- [37] T. Araki and A. Onuki *J. Phys.:Cond. Mat*, vol. 21, p. 424116, 2009.